数理解析研究所講究録 第2128巻 2019年 173-181

京都大学数理解析研究所講究録「非線形波動現象の数理とその応用」

A 3D Numerical Analysis for Tsunamis Ascending a River

Taro Kakinuma* and Yoshimi Kusuhara*

* Graduate School of Science and Engineering, Kagoshima University

1. Introduction

The tsunamis due to the earthquake off the Pacific coasts of the Tohoku region, Japan, caused extensive damage to not only the coastal regions but also the inland areas along the rivers ascended by the tsunamis, in 2011. It should be noted that both the phase velocity and the travelling distance of tsunamis ascending rivers are generally larger than that of tsunamis running up on land. The tsunamis ascended the Kitakami River for about 49 km from its river mouth, while the maximum distance travelled by the tsunamis on the corresponding land area was about 12 km. Roh et al. (2015) developed an estimation method for the tsunami parameters, including river discharge and flow velocity of the Kitakami River. Around the mouths of rivers, the tsunamis broke many tide gates and seawalls, as well as the reefs and lagoons (e.g. Kakinuma et al., 2012). The tsunamis also propagated the Pacific to run up the Columbia River in Canada and the U.S. (Yeh et al., 2012).

Tsunamis ascending a river were observed several times in Japan, owing to the occurrence of submarine earthquakes such as the 1983 Sea of Japan earthquake and the 2003 Tokachi-Oki earthquake, where the tsunamis showed wave disintegration. According to the three-dimensional numerical results obtained by Kusuhara et al. (2018), the tsunami height increases upstream, as the tsunamis show remarkable wave disintegration in the rivers with a narrow width. In the present study, the tsunamis ascending a river have been simulated using a three-dimensional numerical model, to study the effects of uniform river width, river-mouth shape, and river-width decrease, on tsunami-propagation characteristics, including tsunami height.

2. Numerical Method and Conditions

Tsunamis ascending a river are numerically simulated using CADMAS-SURF/3D (Coastal Development Institute of Technology, 2010), where the factors for viscosity, eddy viscosity and friction are neglected for simplicity, such that the fundamental equations are the continuity equation and the Euler equations for inviscid and incompressible fluid motion, where the Poisson pressure equations are also solved numerically.

Shown in Figs. 1 and 2 are the numerical computation domains, where the cross-section shape of the rivers is a rectangle, and the river course is straight. It should be noted that a vertical wall with the perfect-reflection condition for waves, is installed at the center line along the river-course direction, such that the numerical computation domain is half of the target area, owing to the axisymmetry.

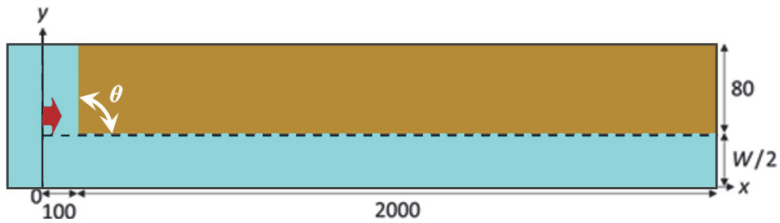

Fig. 1. The computational domain for tsunamis ascending a river with a rectangle cross section, the width of which is uniform. The river width is W, and the angle between the seawall and the river wall is denoted by θ. The incident solitary wave is generated at $x = 0.0$ m. The unit of length is m.

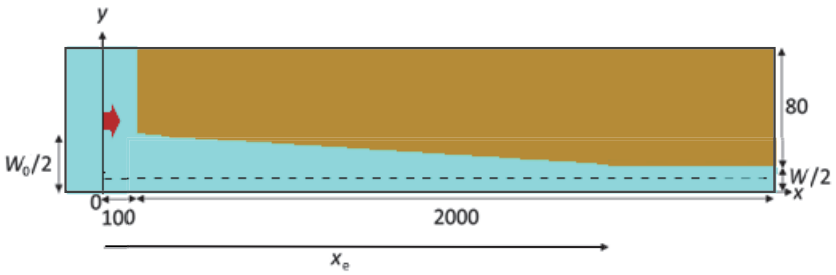

Fig. 2. The computational domain for tsunamis ascending a river with a rectangle cross section, where the river width linearly decreases upstream, from the river mouth at $x = 100.0$ m, to the position of $x = x_e$. The river widths at the river mouth and the upstream end are W_0 and W, respectively. The incident solitary wave is generated at $x = 0.0$ m. The unit of length is m.

The width of the river shown in Fig. 1 is uniform along the river-course direction, while the width of the river shown in Fig. 2 decreases upstream in part of the river. In all the cases, the still water depth is 3.0 m everywhere in both the sea and the river. The effect of river charge on the propagation of tsunamis is neglected for simplicity.

First, the effect of river width W on tsunamis ascending a river is investigated, where the numerical computation domain is the area shown in Fig. 1. Second, although the numerical computation domain is the area shown in Fig. 1, the effect of river-mouth shape on tsunamis ascending a river is studied, for various values of the angle between the seawall and the river wall, θ. Finally, the numerical computation domain is the area shown in Fig. 2, and the effect of decrease in river width on tsunamis ascending a river is examined, for various values of the distance, where the river width decreases upstream.

The water surface elevation in still water is denoted by $z = 0.0$ m, where the upward direction is the positive direction of the vertical coordinate z. The horizontal coordinates are x and y, where the upstream direction is the positive direction of x, and the incident wave is generated at $x = 0.0$ m, while the direction from the left bank to the right bank is the positive direction of y, and the river center in the transverse direction is at $y = 0.0$ m. The grid sizes for the x, y and z directions are $\Delta x = 2.0$ m, $\Delta y = 2.0$ m and $\Delta z = 0.1$ m, respectively, while the time step Δt is automatically decided by

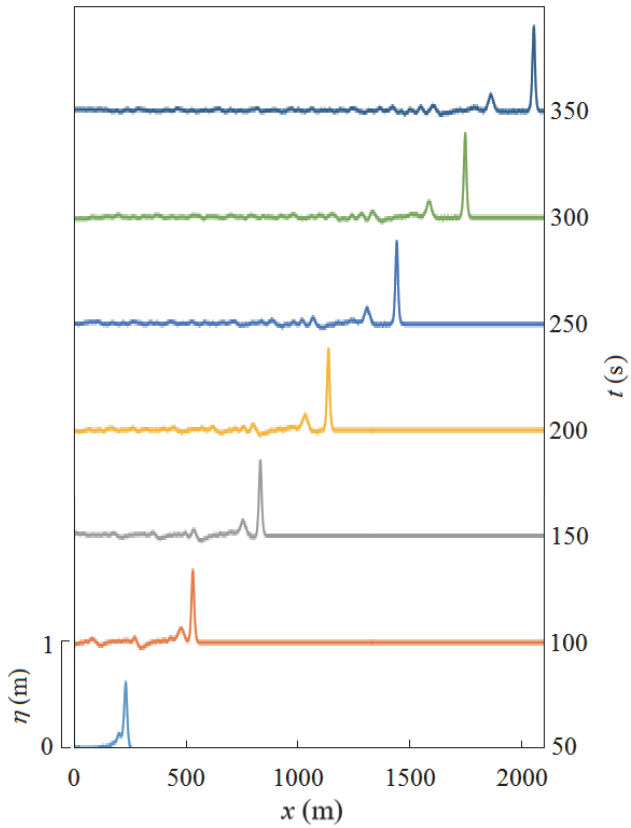

Fig. 3. The time variation of water surface profile along the broken line at $y = W/2$, indicated in Fig. 1, where the tsunamis ascend the river with the uniform river width of $W = 20.0$ m. The water surface displacement is denoted by η, and x is distance from the wave-generated position.

satisfying the CFL condition.

The incident wave is a solitary wave, generated at $x = 0.0$ m in the sea region, where the incident wave height is 0.5 m, uniformly along the y-direction. The Sommerfeld radiation condition is adopted at both the offshore end of the sea, and the upstream end of the river. The perfect reflection condition for waves is utilized at the vertical river walls, as well as the vertical seawalls, the height of which is assumed to be large, such that inundation is not considered in the present study.

3. The effect of uniform river width on tsunamis ascending a river

The effect of river width on tsunamis ascending a river is investigated, where the numerical computation domain is shown in Fig. 1, and the angle between the seawall and the river wall, θ, is 90.0°. Depicted in Fig. 3 is the time variation of water surface profile along the broken line at $y = W/2$, shown in Fig. 1, where the river width W is uniformly 20.0 m, while Fig. 4 shows that for the

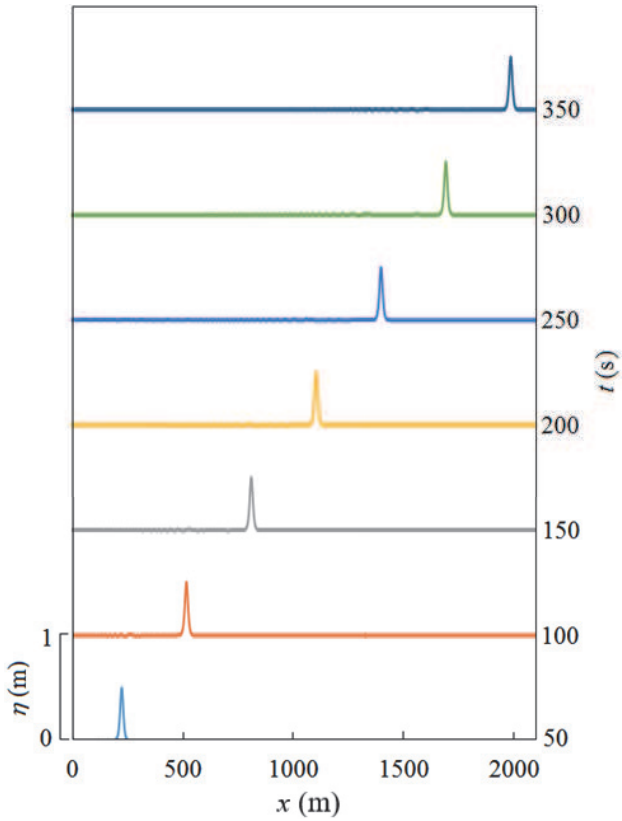

Fig. 4. The time variation of water surface profile at y = 10.0 m in Fig. 1, in the region with the uniform still water depth of 3.0 m, without a land. The water surface displacement is denoted by η, and x is distance from the wave-generated position.

case without a river, where the width of the land shown in Fig. 1 is zero. According to Fig. 4, the incident solitary wave propagates stably without a river. Conversely, according to Fig. 3, the maximum water level, i.e., the tsunami height of the first wave, H, increases, because of the wave disintegration, with the generation of a wave train behind the main wave. It should be noted that the disintegration of tsunamis can also occur in rivers with both a uniform river width and a uniform water depth.

Figure 5 shows the distributions of tsunami height H along the broken line at $y = W/2$, indicated in Fig. 1, where the river width W is 10.0 m, 16.0 m, 20.0 m, 22.0 m, 24.0 m, 30.0 m, 40.0 m, 50.0 m, 60.0 m, 100.0 m and 200.0 m. The tsunami height increases at each position for 300.0 m < x < 1250.0 m, as the uniform river width is decreased. In the cases where the river width W is 10.0 m, 16.0 m and 20.0 m, the tsunami height increases, as the tsunami travels upstream, owing to the wave disintegration as mentioned above. The upper limit of the tsunami height is around 0.8 m in these three cases. In the other cases of $W \geq$ 22.0 m, the tsunamis do not show notable amplification, without remarkable wave disintegration, and the tsunami height decreases upstream, after showing a

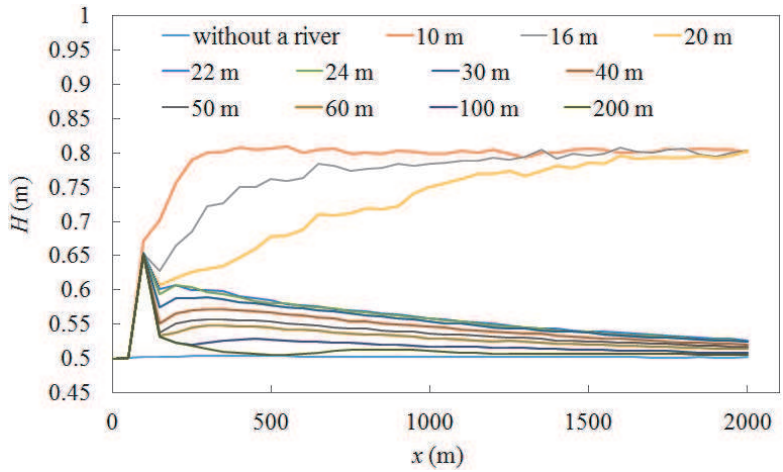

Fig. 5. The distributions of tsunami height H along the broken line at $y = W/2$, indicated in Fig. 1, for various values of river width W, where the tsunamis ascend the rivers of uniform river widths; x is distance from the wave-generated position.

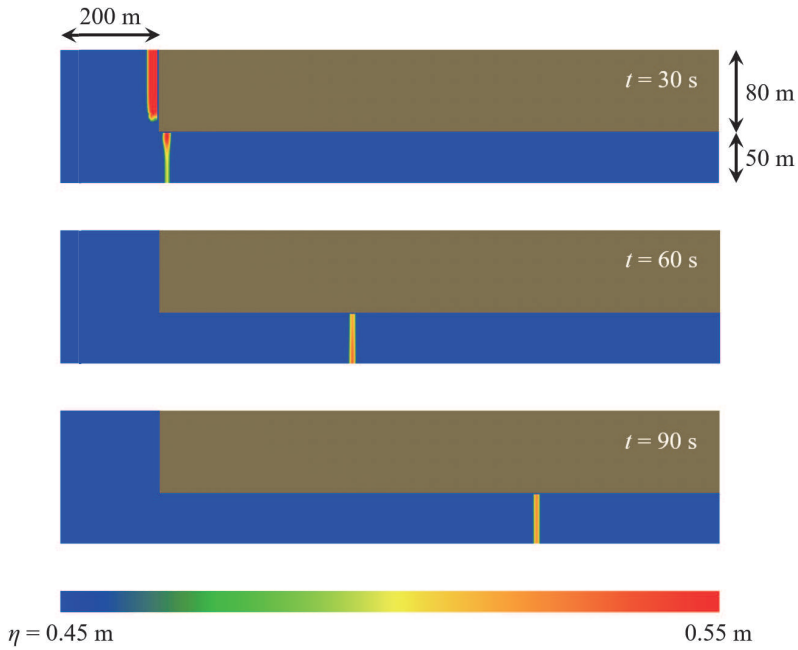

Fig. 6. The distributions of water surface displacement η at t = 30.0 s, 60.0 s and 90.0 s, in part of the computational domain shown in Fig. 1, where the tsunamis ascend the river with the uniform river width of W = 100.0 m.

maximal value for $x > 200.0$ m, where the location of the maximal value depends on the river width.

Shown in Fig. 6 are the distributions of water surface displacement η at t = 30.0 s, 60.0 s and 90.0 s,

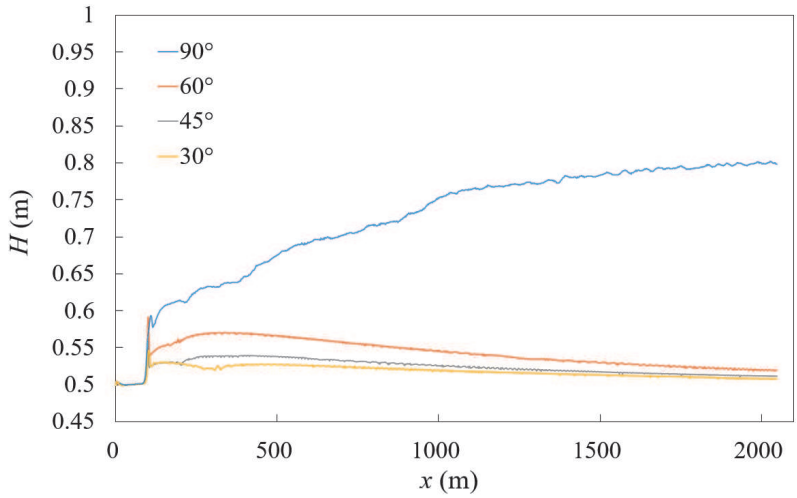

Fig. 7. The distributions of tsunami height H along the broken line at $y = W/2$, indicated in Fig. 1, for various values of the angle between the seawall and the river wall, θ, where the tsunamis ascend the rivers with the uniform river width of $W = 20.0$ m; x is distance from the wave-generated position.

in part of the computational domain shown in Fig. 1, where the tsunamis ascend the river with the uniform river width of $W = 100.0$ m. Although the tsunami height does not show remarkable amplification due to wave disintegration, it increases near the river bank at the river mouth, for the diffracted wave also enters the river. The tsunami height increases near the river center in the transverse direction at $t = 60.0$ s, after which it shows increase near the river bank at $t = 90.0$ s, resulting in the appearance of the maximal value at the river bank, as mentioned above.

4. The effect of river-mouth shape on tsunamis ascending a river

The effect of river-mouth shape on tsunamis ascending a river is studied, for various values of the angle between the seawall and the river wall, θ, where the numerical computation domain is shown in Fig. 1, and the river width W is 20.0 m. Shown in Fig. 7 are the distributions of tsunami height H along the broken line at $y = W/2 = 10.0$ m, indicated in Fig. 1, where $\theta = 30.0°$, 45.0°, 60.0° and 90.0°. When θ is less than 90.0°, the diffracted wave with less energy enters the river, such that the tsunamis do not show remarkable amplification due to wave disintegration in the present cases.

5. The effect of decrease in river width on tsunamis ascending a river

The effect of decrease in river width on tsunamis ascending a river is examined, for various values of the distance, where the river width linearly decreases upstream. The numerical computation domain is shown in Fig.2, where the river width at the river mouth, W_0, is 200.0 m. The river width linearly decreases upstream, from the river mouth at $x = 100.0$ m, to the position of $x = x_e$, where x_e = 1400.0 m, 1500.0 m, 1600.0 m and 2100.0 m, and the river width at the upstream end is 83.0 m,

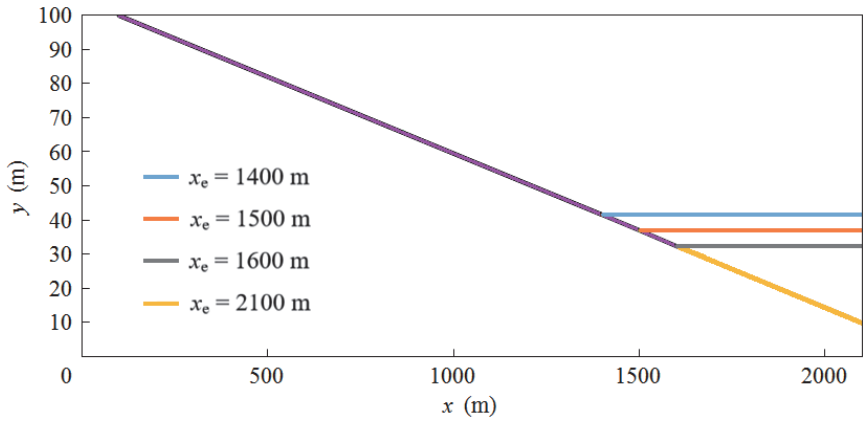

Fig. 8. The right-bank configurations of the rivers ascended by the tsunamis, for various values of the distance, where the river width linearly decreases upstream, from the river mouth at x = 100.0 m, to the position of $x = x_e$, where x_e = 1400.0 m, 1500.0 m, 1600.0 m and 2100.0 m, and the river width for $x \geq x_e$ is 83.0 m, 74.0 m, 65.0 m and 20.0 m, respectively; x is distance from the wave-generated position.

74.0 m, 65.0 m and 20.0 m, respectively. The right-bank configurations for these cases are drawn in Fig. 8.

Figure 9 shows the distributions of tsunami height H along the broken line at y = 10.0 m, indicated in Fig. 2. When x_e is 2100.0 m, where the river width linearly decreases from the river mouth to the upstream end, the tsunami height becomes larger than 0.6 m at x = 1470.0 m, and it shows remarkable increase upstream, after the tsunami passes the position of x = 1500.0 m, resulting in the tsunami height, which is almost twice as large as the incident wave height, at x = 2000.0 m. This notable increase in tsunami height is due to both the decrease in the river width, and the wave disintegration after the tsunami passing the position of x = 1500.0 m, where the river width is 74.0 m. It should be noted that remarkable wave disintegration does not occur with the uniform river width of 74.0 m, according to Fig. 5. When x_e is 1600.0 m, although the tsunami height shows remarkable increase after the tsunami passes the position of x = 1500.0 m, the tsunami height remains constant at 0.7 m for $x \geq$ 1600.0 m, where the river width is uniformly 65.0 m. When x_e is 1500.0 m, the tsunami height also increases remarkably, after the tsunami passes the position of x = 1500.0 m, but the tsunami height decreases for $x \geq$ 1560.0 m, where the river width is 74.0 m. Conversely, when x_e is 1400.0 m, the tsunami does not show remarkable wave disintegration, such that the tsunami height decreases upstream, after the tsunami passes the position of x = 1460.0 m, where the river width is 83.0 m.

6. Conclusions

The tsunamis ascending the rivers were simulated, using the three-dimensional numerical model. The maximum water level at each position, i.e., the tsunami height, increased, as the uniform river

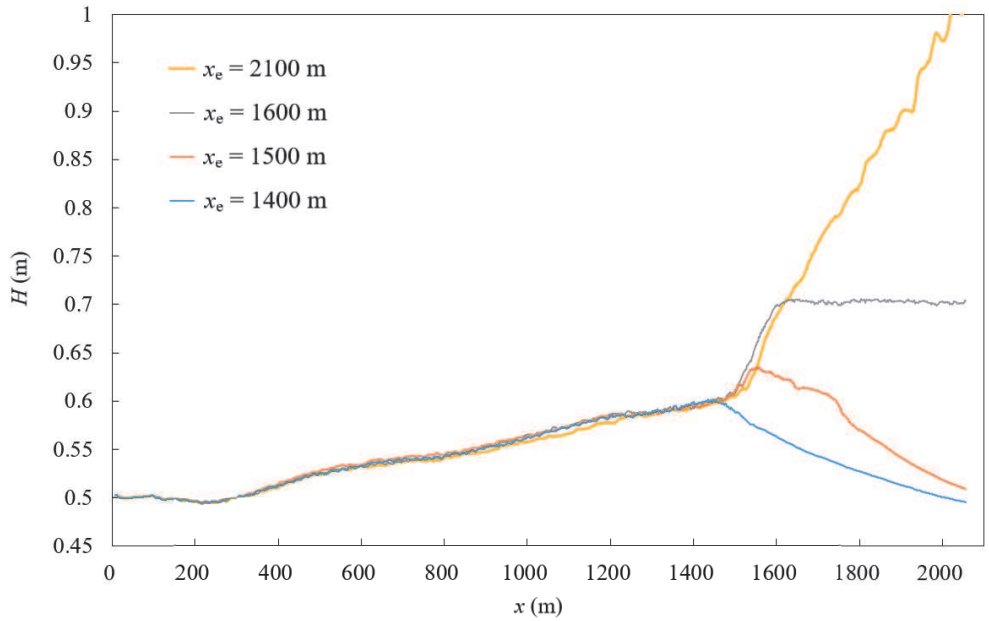

Fig. 9. The distributions of tsunami height H along the broken line at y = 10.0 m, indicated in Fig. 2, for various values of the distance, where the river width linearly decreases upstream, from the river mouth at x = 100.0 m, to the position of $x = x_e$; x is distance from the wave-generated position. The right-bank configurations of the rivers are drawn in Fig. 8.

width was decreased. When the tsunamis show notable wave disintegration in the narrow rivers, the tsunami height showed remarkable increase upstream. Conversely, without remarkable wave disintegration in the wide rivers, the tsunami height decreased upstream, after showing a maximal value, the location of which depended on the river width. When the angle between the seawall and the river wall is an acute angle, the diffracted wave with less energy entered the river, such that the tsunamis did not show amplification due to wave disintegration, in the present cases. In the cases determining the tsunamis ascending a river with river width decreasing upstream in part of the river, when the river width is decreased enough, the tsunami height did not decrease upstream, owing to the wave disintegration.

Acknowledgments

This work was supported by the aid fund from Yonemori Seishin Ikuseikai.

References

Coastal Development Institute of Technology: CADMAS-SURF/3D, Coastal Development Library, No. 39, 235p., 2010 (in Japanese).

Kakinuma, T., Tsujimoto, G., Yasuda, T. and Tamada, T.: Trace survey of the 2011 Tohoku Tsunami in the north of Miyagi Prefecture and numerical simulation of bidirectional tsunamis in Utatsusaki Peninsula, Coastal Eng. J., Vol. 54, No. 1, Article ID 125007, 28p., 2012.

Kusuhara, Y., Kakinuma, T. and Kimura, A.: A 3D Numerical study for the characteristics of tsunamis ascending rivers, J. JSCE, Ser. B2 (Coastal Eng.), Vol. 74, Issue 2, pp. I_199-I_204, 2018 (in Japanese with an English abstract).

Roh, M., Adityawan, M. B. and Tanaka, H.: Assessment of propagation characteristics for tsunami wave ascending river, In: Coastal Eng. 2014 (Ed. Lynett, P. J.), currents. 19, 9p., 2015.

Yeh, H., Tolkova, E., Jay, D., Talke, S. and Fritz, H.: Tsunami hydrodynamics in the Columbia River, J. Disaster Res., Vol. 7, pp. 604-608, 2012.